REKAYASA 22 (2) (2024): 97-107

REKAYASA

Jurnal Penerapan Teknologi dan Pembelajaran

http://journal.unnes.ac.id/journals/rekayasa

Analyzing the Total Resistance and Wave Pattern of Purse Seine Vessels with Photovoltaic-Powered

Rizqi Fitri Naryanto*[1], Aldias Bahatmaka[1], Muhammad Yusuf Wibowo[1], Andi Abdullah Ghyferi[1], Fiqri Fadillah Fahmi[1], Joung Hyoung Cho[2]

[1]Mechanical Engineering Study Program, Universitas Negeri Semarang, Semarang, Indonesia

[2]Marine Design Convergence Interdisciplinary Program, Pukyong National University, Busan, South Korea

*Email: rizqi_fitri@mail.unnes.ac.id

DOI: https://doi.org/10.15294/rekayasa.v22i2.10634

Abstract

With 64.97% of its territory consisting of sea, Indonesia is one of the world's largest maritime nations and produces approximately 8.02 million tons of fish annually. Traditional fishing vessels play a crucial role in supporting livelihoods, yet their design is often based on hereditary methods rather than hydrodynamic optimization. This study uses catamaran hull forms as a design reference to analyze the total resistance and wave patterns of purse seine vessels with photovoltaic-powered systems. Computational methods are employed to predict vessel performance efficiently. The resistance analysis applies the Slender Body approach and Savitsky's mathematical model, supported by comparative studies for validation. Particular attention is given to the influence of chine configurations on resistance characteristics and wave formation. Results indicate that the addition of chines increases the Froude number and contributes to reducing total resistance. Among the variations, single chine geometry demonstrates the lowest resistance, making it the most efficient configuration for catamaran fishing vessels. While chine modifications affect the wave pattern, the hull maintains a relatively clean wake distribution. These findings highlight the potential for improving vessel design through careful chine geometry optimization combined with computational modeling. The study underscores the importance of modern hydrodynamic analysis in advancing traditional fishing vessels toward higher efficiency and sustainability. Future research is recommended to incorporate more advanced computational approaches, such as Computational Fluid Dynamics (CFD), examine water-hull interactions and enhance vessel performance under operational conditions

Keywords: catamaran hull, computational approach, fishing, ship design, transportation.

INTRODUCTION

Indonesia is located between the Pacific Ocean and the Indian Ocean. In addition, Indonesia is a maritime country, with data indicating that Indonesia's sea area comprises 64.97% of the country's total territory

(Pudjiastuti et al., 2021). The Indonesian oceans, located in tropical climates, carry the consequences of species wealth and potential fishery resources, for example, fish are estimated to have 6,000 species and only 3,000 species have been identified (Sasvia, 2019). In Indonesia's seas, there are differences in wave conditions in each region, especially in rainfall. During the rainy season, the conditions of the high sea waves make fishermen fish in the sea (Hafsaridewi et al., 2020). Flooding in Indonesia is complex due to seabed topography, coastline shape, and the interaction of the Pacific, Indian, and South China Seas (Noor & Abdul Maulud, 2022). These wave differences result in the vessel's shape adjustment to match the waves in a particular region. Traditional fishing vessels are manufactured in Indonesia using skills passed down from generation to generation and are one of the ways of transportation and livelihood (Bahatmaka & Kim, 2019). Therefore, in this particular case, it is important to measure and assess the fishing vessel model's shape in terms of the characteristics of the Indonesian Sea (Liu et al., 2019).

Indonesia's fishing industry is vital for food security and employment, but it requires efficient and eco-friendly vessels to lower costs and environmental impact. The conventional technique of fish storage leads to unfavourable conditions that damage the quality of the fish catch (Tavares et al., 2021). Creating fishing boats with the RSW cold store snorkel and Light Fishing Reflectors based on photovoltaic energy has become a successful answer to such questions. In the RSW system, the fish storage compartment is isolated with a vacuum to keep the temperature constant and to reduce internal and external temperature differences (Anders et al., 2023). It assists in freshness and quality enhancement and minimizes fish spoilage and the duration that fish can stay in the market and still be saleable (Siddiqui et al., 2024; Alam et al., 2015).

Besides proper fish storage, using Light Fishing Reflectors connected to photovoltaic sources is highly advantageous for preserving the sustainable fishing approach (Mulyono et al., 2023). This lighting system uses LED lights to apply reflectors on a fishing net, dramatically impacting fishing since it attracts the fish. As renewable sources of energy, these photovoltaic systems help in decreasing the demand for scarce non-renewable sources of energy, hence minimizing operational costs, and by so doing bring down the impacts associated with fishing expeditions (Al Mubarak et al., 2024; Muir, 2015). The use of renewable energy in fishing vessels is increasingly discussed due to fossil fuel depletion and environmental impacts that threaten fisheries' sustainability (Koričan et al., 2023). Thus, the following paper aims to focus on such intensified systems, consider the ways of their design and application, and emphasize the satisfactory results and benefits of their implementation in the fishing industry.

When a ship is above sea level, it will always gain strength from the outside of the ship, which causes the ship to move. This ship's movement is caused by external factors, mainly by waves (Bahatmaka et al., 2023). Excessive movement of the ship during operation causes uncomfortable conditions for the ship's crew, such as being drunk or bouncing and disturbing the crew while performing activities on the ship. This problem will limit the vessel's capability and duration of operations, especially when there is a considerable wave (Afdhal et al., 2019). When the ship is above the wave, it will experience the worst hogging load at the moment when the middle position of the ship's body is over the peak of the wave crest, while on the bow and the stern, it is in the wave trough. Therefore, it is necessary to design a

ship that can survive in all conditions of the catamaran hull type.

Catamaran vessels are widely used due to the availability of a wider deck area and a more comfortable and safe level of stability (Julianto et al., 2020). In addition, a catamaran with a thin body shape (slender) can reduce the appearance of a wave wash compared to a mono-hull ship. Calculations and computations are performed using the Maxsurf program to determine the barrier ship's interference on the catamaran hull (Pratama et al., 2023). The shape coefficient of the catamaran is greater than its demi hull due to the presence of z effects, where the difference between the two can reach 10%. Another factor that needs to be considered in the ship's design is strength due to the presence of combined loads to know the reaction of structures on the ship (Siagian et al., 2020).

In addition, the catamaran has a more attractive accommodation layout, improved transversal stability and can sometimes decrease the ship's propulsion to a certain service speed (Xing-Kaeding & Papanikolaou, 2021). The size of the catamaran ship can make it easier for designers to make it more convenient to arrange the accommodation space of the ship (Iqbal et al., 2020). Because the generated obstacles are minor, catamaran ships have higher speeds and lower ship loads, resulting in small operating costs. The guaranteed safety impact of the reversed ship factor can also be found on catamaran ships (Shi et al., 2021). Both demihulls on the catamaran ship are arranged with bridging networks. This bridging structure is a catamaran advantage because it increases the height of the hull (freeboard), so the likelihood of deck wetness can be reduced, and the ship is also able to operate in shallow waters (Pérez Fernández & González Redondo, 2022).

Resistance is key to ship analysis, determining how effectively a vessel can function hydrodynamically (Ohwofadjeke et al., 2024). The water that goes through the hull as it moves forward and crosses the sea will provide resistance. Research is needed to determine whether the ship should be built to go through the water with the least amount of external force possible (Bilgili, 2023). Resistance is affected by factors including ship speed (Vs), displacement, and hull type. There are two types of resistance force: normal and tangential. The normal force (Fn) acts perpendicular to the hull surface, while the tangential force (Ft) acts parallel to the hull surface. Both of these forces contribute to the frictional resistance experienced by the vessel, as shown in Equation (1), where: R_T is total resistance (N), R_F is frictional resistance (N), R_V is viscous resistance (N), and R_W is wave resistance (N).

$$R_T = R_F + R_V + R_W \quad (1)$$

The force used to press the surfaces together is usually directly proportional to the frictional resistance. The portion of the applied force that works perpendicularly or normally to the surface is the force that will affect frictional resistance. The International Towing Tank Conference (ITTC) of 1975 provided the friction coefficient as Equation (2) and Equation (3), where Cf is the friction coefficient, S is the wetted surface area (m^2), V is the velocity (m/s), and Re is the Reynolds number.

$$R_f = \frac{1}{2} \rho C_f . S . V^2 \quad (2)$$

$$Cf = \frac{0.075}{(Log\ Re - 2)2} \quad (3)$$

Viscous resistance, as described by Zeng et al. (2019), is the resistance caused by the viscous forces that a fluid places on a ship's body. The amount of viscous resistance is

typically based on the form factor (1+k) for mono-hulls shown in Equation (4), where Cv is the viscous resistance coefficient, k is the form factor, and β is = multi-hull correction factor.

$$C_v = (1+k)\, C_f \quad (4)$$

Wave resistance is a type of drag that affects surface vehicles like boats and ships (Kumar et al., 2020). Due to minimal resistance values, the wave resistance is zero at high speed (Vs). It is seen in Equation (5), where Rw is wave resistance (N), C_1, C_2, C_5, m_1, m_2, λ are the empirical coefficients, ∇ is displacement volume (m^3), ϱ is water density (kg/m^3), g is gravitational acceleration (m/s^2), and F_n is the Froude number.

$$R_w = C_1 C_2 C_5 \nabla.\varrho\, g \exp\{m_1 f_n^d + m_2 \cos(\lambda F_n^{-2})\} \quad (5)$$

Reynolds' number will determine the fluid's shape. The Reynolds number determines a fluid's laminar or turbulent behaviour (Saldana et al., 2024). The Reynolds' number equation represents the ratio between the force of inertia and viscosity. It is evident in Equation (6), where V is fluid speed, L is characteristic length, and v is kinematic viscosity. Laminar flow has a Reynolds' number value of between 2300 and 4000.

$$R_e = \frac{V.\ L}{v} \quad (6)$$

The Froude number indicates the speed compared to the mass displaced. In hydrodynamics, the Froude number represents a specific model that works for a system. A Froude number can be called a semi-displacement if its value is around 0.4 to 1. However, if the value is above 1, it is called a planning hull. It can be seen in the Equation (7) .

$$F_n = \frac{V}{v} \quad (7)$$

The wetted surface area can be computed using Mumford's formula to suggest an error rate of around 7%. Utilizing the setups for measuring the type of ships can increase accuracy (Dudojc & Mindykowski, 2019). The wetted surface area has an impact on the resistance. The wetted surface area can be calculated using Equation (8), where S is the wetted surface area, L_{pp} is the length between perpendiculars, Cb is the block coefficient, b is the beam, and T is the draft.

$$S = 1.025.\ L_{pp}.\ (C_b.b + 1.7T) \quad (8)$$

Savitsky's mathematical model is utilised in calculations to determine the wet areas, drag, pressure, stability, and resistance, which may be employed as a function of speed, deadrise angle, and trim in the hydrodynamic parameters for a numerical approach. The empirical formula for prismatic planning hull is shown in Equation (9), where Δ is displacement, and τ is trim angle.

$$RT = \Delta \tan \tau \frac{\frac{1}{2}\rho V^2 \lambda b^2 C_f}{\cos \tau} \quad (9)$$

The slender body approach considers the vessel's slenderness by assuming high length-to-beam or slenderness ratios. Although the slenderness ratio should ideally be as high as feasible, in practical terms, slenderness ratios between 5.0 and 6.0 might produce satisfactory outcomes. The minimal slenderness ratio to which the approach is applicable likewise decreases as the vessel's Froude number increases. The vessel's slenderness ratio determines the most significant Froude number for which reasonable results can be achieved. It has been discovered that the slender body

approach may get accurate findings for Froude values as high as 1.0 for very slender vessels (slenderness ratios greater than 7.0). Round bilge and chine hull types are equally amenable to the low-profile approach. Transom stern hulls are handled by a "virtual appendage" being automatically added. The demihull slenderness ratio, L/∇1/3 to calculate the form factor in the following Equation (10), where (1+βk) for multi-hulls.the viscous.

$$(1+ \beta k) = 3.03 (L/\nabla^{1/3})^{-0.40} \quad (10)$$

METHOD

This study focused on improving fishing vessel catamaran hull design and hull comparative analysis by selecting the most effective designs and having the best performance among those designs. This analysis process follows the rules applicable at MARINESIA 2023 (Indonesian Marine Innovation Festival) competition to measure the size of the ship. The fishing vessel is selected as the research object using linear regression of the selected reference vessel. The reference vessels selected can be seen in Table 1. In this process, the ratio of the vessels of the Long/Breadth ratio (L/B), Long/Height ratio, and Breadth/Draft (B/T) ratio is found. The vessel size obtained for the new design is presented in Table 2, and the design of its vessel lines plan is shown in Figure 1a and 1b.

The numerical simulations were performed using Maxsurf software with a computational domain defined as open sea conditions. Mesh convergence was achieved using an average cell size of 0.2 m. The simulations were conducted at vessel speeds corresponding to Froude numbers ranging from 0.153 to 0.267. The physical properties of seawater were defined according to ITTC (1975) standards, with density 1025.9 kg/m³, kinematic viscosity 1.1×10^{-6} m²/s, salinity 3.5%, and gravitational acceleration 9.8 m/s².

Table 1. Reference Dimension of Ship

Type of Ships	Dimension							
	LOA	**LPP**	**B**	**H**	**T**	**L/B**	**L/H**	**B/T**
MAREEL VERDIGRIS	76.50	69.00	22.50	9.00	4.59	3.07	8.50	4.90
MAREEL VIOLET	75.00	67.50	22.50	10.50	4.50	3.00	7.14	5.00
MARINER	78.00	69.00	25.50	12.00	6.00	2.71	6.50	4.25
MASTER	78.60	72.00	26.79	12.00	6.00	2.70	6.55	4.47
SEACAT COURAGEOUS	78.90	66.00	26.85	10.80	4.50	2.69	7.31	5.97
SEACAT INTREPID	78.00	67.50	26.85	10.80	4.50	2.69	7.22	5.97
WEM 3	81.00	72.00	24.00	12.00	8.40	3.00	6.75	2.86

Table 2. Main Dimension of the New Design

Dimension	Notation	Value (m)
Length Overall	L_{OA}	78
Length Between Perpendicular	L_{BP}	69
Breadth	B	25
Height	H	11
Draft	T	5.5

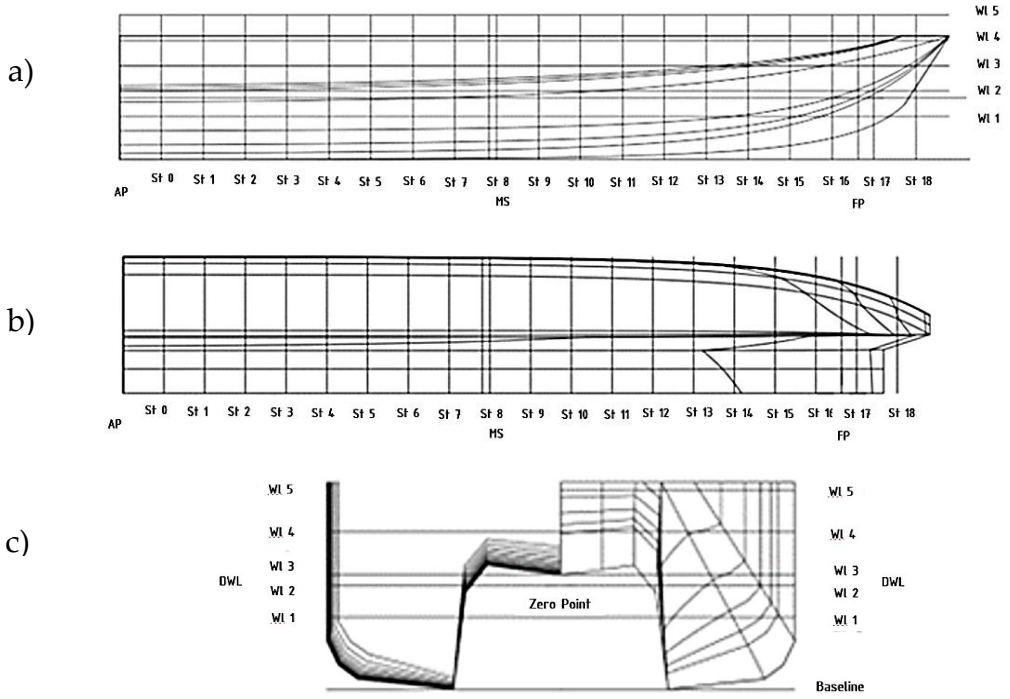

Figure 1. The Ship Design of (a). Sheer Plan, (b). Half Breadth Plan, (c) Body Plan

Numerical Configuration and Benchmarking Study

The ship's hydrostatic data is used in this chapter as a configuration variable. Table 3 shows the characteristics of the new design. The ship's speed is variably controlled with an 8 Knot minimum speed and a 14 Knot maximum speed. Seawater must have a salinity of 3.5%, a kinematic viscosity of 0.0000011 m^2/s, a density of 1025.9 kg/m^3, a gravity of 9.8 m/s^2, and a temperature of 15°C, according to the ITTC 1975. Savitsky and Slender Body methods were applied as benchmarking approaches to analyze the resistance characteristics of the new catamaran design (Adiba & Kurniawati, 2016). The Savitsky method is generally suitable for planning hulls, while the Slender Body method provides accurate predictions for slender catamaran hulls at low to medium Froude numbers. As shown in Figure 2, the two methods present consistent results, thereby validating the accuracy of the resistance analysis. This research's resistance analysis compares the characteristics resulting from the designs' effects. For the purpose of estimating the power required by the ship design, low resistance may be projected. As a result, various parameters and scenarios have been explored using different ship speeds and Froude numbers. The summary of the resistance comparisons is shown in Table 4.

Design Variation

The study focused on the effect of chine variations across four different speeds. Figure 3 illustrates the chine designs applied in this study: Figure 3a shows the bare hull without a chine, Figure 3b shows the single-chine configuration, and Figure 3c shows the double-chine configuration. The green line in each figure clearly represents the vessel's designed waterline. These configurations were systematically compared to evaluate their influence on total resistance and the resulting wave patterns at different Froude numbers. The main objective was to assess whether increasing the number of chines effectively reduces the total resistance of fishing vessels.

Table 3. Data and Design Characteristics of the New Design

Parameters	Value	Unit	Savitsky	Slender Body
LWL	74.21	m	74.21	74.21
Beam	25	m	25	25
Draft	5.5	m	--	5.5
Displaced volume	4145.53	m^3	4145.53	4145.53
Wetted area	2190.44	m^2	--	2190.44
1/2 angle of entrance	38.4	deg.	--	38.4
LCG from midships (+ve for'd)	-4.14	m	-414	--
Deadrise at 50% LWL	8.7	deg.	8.7	--
Kinematic viscosity	0.0000011	m^2/s	0.0000011	0.0000011
Water Density	1025.90	kg/m^3	1025.90	1025.90

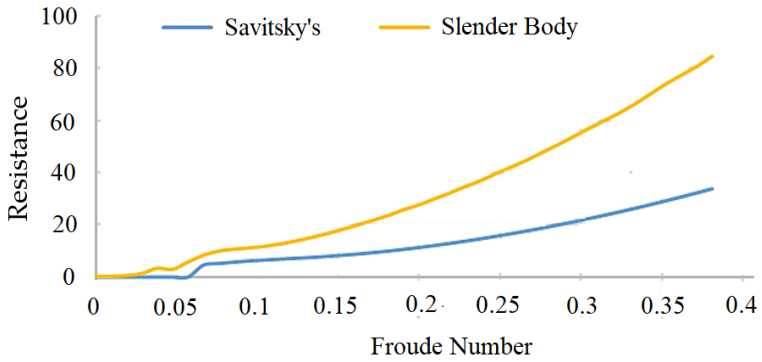

Figure 2. Comparison Method of Total Resistance of Savitsky vs Slender Body

Table 4. Total Resistance Comparison

Fn (-)	V (knot)	Savitsky (kN)	Slender Body (kN)
0.153	8	8.28	18.04
0.191	10	10.54	25.61
0.229	12	13.66	34.49
0.267	14	17.56	44.65

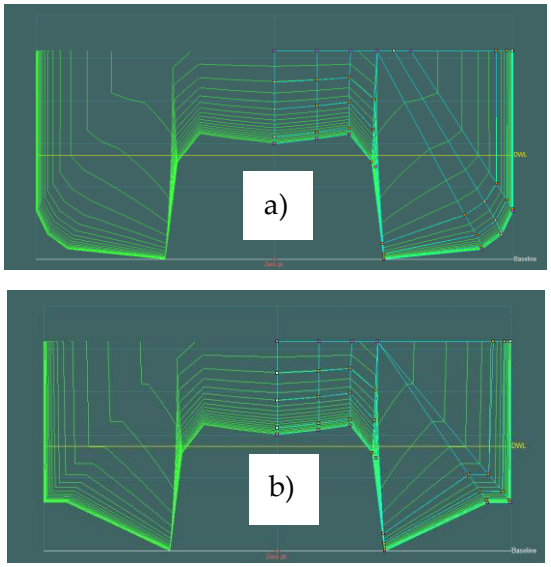

Figure 3. Variation of chine design of (a) Barehull, (b) Single Chine 0°, (c) Double Chine 0°

RESULT AND DISCUSSION

Total Resistance

Table 5 presents the total resistance values of the bare hull, single chine, and double chine configurations at different Froude numbers (Fn). The results show that the bare hull consistently exhibits the highest resistance across all Froude numbers, ranging from 18.04 kN at Fn = 0.153 to 44.65 kN at Fn = 0.267 (Moonesun et al., 2015). In contrast, the single chine hull records the lowest resistance values, with a minimum of 15.78 kN at Fn = 0.153. As the Froude number increases, the resistance difference between the single and double chine configurations narrows, with the double chine showing a slight advantage at higher speeds. For example, at Fn = 0.267, the resistance of the double chine hull is 41.74 kN compared to 41.19 kN for the single chine (Elaghbash et al., 2021).

The analysis indicates that the single chine hull is more efficient at lower Froude numbers due to its ability to produce a stable flow pattern with reduced turbulence, thereby lowering resistance (Riyadi & Suastika, 2020). At higher Froude numbers, however, the double chine hull becomes more favorable, as the additional chine edges distribute hydrodynamic pressure more evenly along the hull surface, effectively reducing drag at increased speeds (Wheeler et al., 2021). Figure 4 illustrates the comparison of total resistance among the three hull configurations, highlighting the shift in performance between single and double chine designs.

Wave Pattern Contour

The ship's Froude number was first assigned, and although its effect was minor, slight changes in the observed wave pattern were identified. The wave contour clearly shows how hull geometry strongly shapes wave formation and overall energy distribution (Elaghbash et al., 2021). Chine variations alter the interaction between bow and stern waves, significantly affecting resistance, fuel efficiency, onboard comfort, and overall vessel stability (Riyadi & Suastika, 2020). Wave crest and trough distribution also strongly influences vessel operability, particularly in crowded fishing areas with dynamic environmental conditions. Therefore, analyzing wave contours is critically important for assessing hydrodynamic performance and practical vessel operability. The chine arrangements are shown in Figure 5 (a–c). At low Froude numbers or in the planing phase, waves appear smoother, reducing resistance and improving vessel stability. However, stronger wave interactions at higher Fn often increase drag and reduce overall hydrodynamic energy efficiency (Zhu et al., 2019).

By combining photovoltaic-powered systems with optimized catamaran hulls, this study promotes greater energy efficiency, reduced emissions, and sustainable fisheries (Wheeler et al., 2021), thereby supporting Indonesia's gradual transition toward a resilient, adaptive, and greener maritime sector.

Table 5. Result of the Total Resistance from Variations of Chine

Fn	Total Resistance from variations of Chine (kN)		
	Barehull	Single Chine	Double Chine
0.153	18.04	15.78	16.08
0.191	25.61	23.05	23.42
0.229	34.49	31.52	31.97
0.267	44.65	41.19	41.74

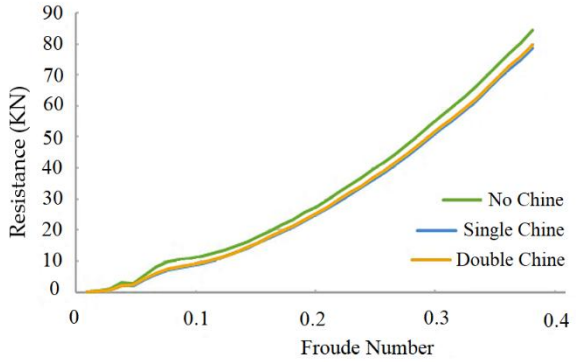

Figure 4. Total Resistance Each Model Variation

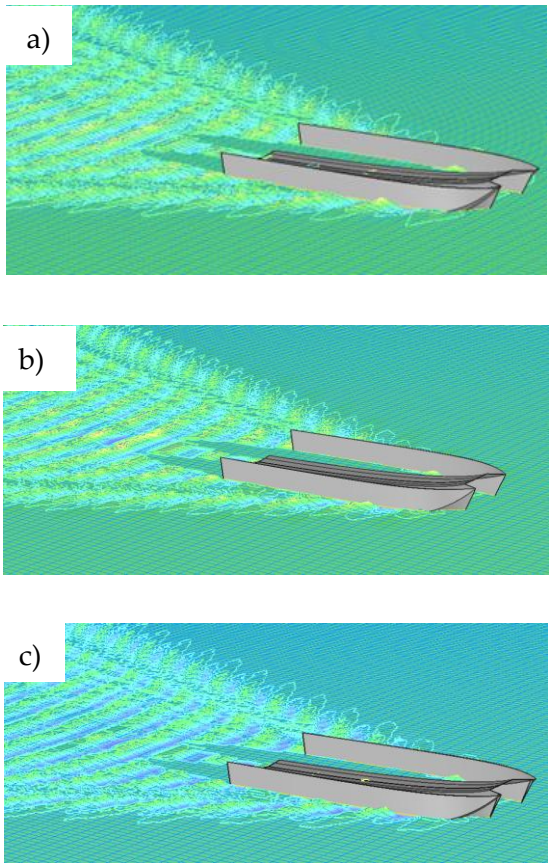

Figure 5. The Wave Pattern of Variations Hull Chine of (a) Barehull, (b) Single Chine 0°, (c) Double Chine 0°

CONCLUSION

The computational result shows that the Slender Body method's approval of the resistance characteristics was successful compared to the Savitsky method. The trend line is also in identical circumstances, and good agreement is shown for all suggested dimensions. Several chines for the catamaran fishing vessel designs were suggested to measure the resistance profile and wave pattern. According to the results, the chine increases the Froude number, reducing overall resistance; for this design, the single chine is the lowest resistance value. Despite a clean pattern surrounding the hull, a change in chine modifies the wave pattern. This research can be strengthened by contrasting a different computational approach to determine how the water interacts with the hull.

REFERENCES

Adiba, N. F., & Kurniawati, H. A. (2016). Desain Trash Skimmer Amphibi-Boat di Sungai Ciliwung Jakarta. *Jurnal Teknik ITS*, *5*(2), 60–65.

Afdhal, M. I., Budiarto, U., & Mulyatno, I. P. (2019). Optimasi Disain Spread Mooring Dengan Konfigurasi Variasi Line Terhadap Six Degrees Of Freedom (DOF) Olah Gerak Pada Kapal Floating Storage And Offloading (FSO). *Jurnal Teknik Perkapalan*, *7*(1), 81-92.

Alam, A. N. (2015). Hygienic Dried and Salted Fish Production-A Field Guide. *WorldFish Centre*, 63.

Al Mubarak, F., Rezaee, R., & Wood, D. A. (2024). Economic, societal, and environmental impacts of available energy sources: A review. *Eng*, *5*(3), 1232-1265.

Anders, N., Breen, M., Skåra, T., Roth, B., & Sone, I. (2023). Effects of capture-related stress and pre-freezing holding in refrigerated sea water (RSW) on the muscle quality and storage stability of Atlantic mackerel (Scomber scombrus) during subsequent frozen storage. *Food Chemistry*, *405*, 134819.

Bahatmaka, A., & Kim, D.-J. (2019). Numerical approach for the traditional fishing vessel analysis of resistance by CFD. Journal of Engineering Science and Technology, 14(1), 207–217.

Bahatmaka, A., Wibowo, M. Y., Ghyfery, A. A., Harits, M., Anis, S., Fitriyana, D. F., ... & Joon, K. D. (2023). Numerical Approach of Fishing Vessel Hull Form to Measure Resistance Profile and Wave Pattern of Mono-Hull Design. *Journal of Advanced Research in Fluid Mechanics and Thermal Sciences*, *104*(1), 1-11.

Bilgili, L. (2023). Determination of the weights of external conditions for ship resistance.*Ocean Engineering*, *276*, 114141.

Dudojc, B., & Mindykowski, J. (2019). New approach to analysis of selected measurement and monitoring systems solutions in ship technology. *Sensors*, *19*(8), 1775.

Elaghbash, A. O. (2021). A CFD study of the resistance behavior of a planing hull in restricted waterways. *Sustainable Marine Structures*, *3*(1), 32-55.

Hafsaridewi, R., Hikmah, H., Zulham, A., Soejarwo, P. A., & Yanti, B. V. I. (2020). Fishers' resilience towards extreme weather conditions in the South China Sea: A case study of Natuna Islands, Indonesia. *Omni-Akuatika*, *16*(3), 49-60.

Iqbal, M., Manik, P., Hadi, E. S., & Kurniawan, A. (2020). Pengaruh Posisi Centerbulb Berbentuk Foil Terhadap Komponen Hambatan Kapal Ikan Katamaran MV. Laganbar. *Jurnal Integrasi*, *12*(1), 64-71.

Julianto, R. I., Muttaqie, T., Adiputra, R., Hadi, S., Hidajata, R. L. L. G., & Prabowo, A. R. (2020). Hydrodynamic and structural investigations of catamaran design. *Procedia Structural Integrity*, 27, 93–100.

Koričan, M., Frković, L., & Vladimir, N. (2023). Electrification of fishing vessels and their integration into isolated energy systems with a high share of renewables. *Journal of cleaner production*, *425*, 138997.

Kumar, S., Verma, K. A., Pandey, K. M., & Sharma, K. K. (2020). A review on methods used to reduce drag of the ship hulls to improve hydrodynamic characteristics. *International Journal of Hydromechatronics*, *3*(4), 297-312.

Liu, W., Demirel, Y. K., Djatmiko, E. B., Nugroho, S., Tezdogan, T., Kurt, R. E., ... & Incecik, A. (2019). Bilge keel design for the traditional fishing boats of Indonesia's East Java. *International Journal of Naval Architecture and Ocean Engineering*, *11*(1), 380-395.

Mulyono, R. D. A. P., Mahardiyanto, A., Afandi, M. F., Aprillianto, B., & Komariyah, S. (2023). Commercalization of Sun-Based Fishing Lights to Improve the Fisherman's Economy in the Horse Area, East Java, Indonesia. *International Journal of Current Science Research and Review*, *6*(09), 6214-6221.

Muir, J. F. (2015). Fuel and energy use in the fisheries sector: Approaches, inventories and strategic implications. *FAO Fisheries and Aquaculture Circular*, 1080.

Moonesun, M., Korol, Y., & Dalayeli, H. (2015). CFD analysis on the bare hull form of submarines for minimizing the resistance. *International Journal of Maritime Technology*, *3*, 1-16.

Noor, N. M., & Abdul Maulud, K. N. (2022).

Coastal vulnerability: a brief review on integrated assessment in Southeast Asia. *Journal of Marine Science and Engineering*, *10*(5), 595.

Ohwofadjeke, P. O., Udo, A. E., & Jonah, J. O. (2024). Characterization of fluid-structure interaction on hydrodynamic performance of different ship hulls using ANSYS. *Computational Engineering and Physical Modeling*, *7*(1), 12-32.

Pérez Fernández, R., & González Redondo, F. A. (2022). On the origin, foundational designs and first manufacture of the modern catamaran. *International journal of maritime history*, *34*(3), 467-493.

Pratama, A. S., Prabowo, A. R., Tuswan, T., Adiputra, R., Muhayat, N., Cao, B., ... & Yaningsih, I. (2023). Fast patrol boat hull design concepts on hydrodynamic performances and survivability evaluation. *Journal of Applied Engineering Science*, *21*(2), 501-531.

Pudjiastuti, E. T., Putra, I. N., & Susilo, A. K. (2021). Vision of the world maritime axis of indonesia as a maritime country in alfred thayer mahan's perspective. *Journal of Defense Resources Management*, *12*(2), 211-219.

Riyadi, S., & Suastika, K. (2020). Experimental and numerical study of high froude-number resistance of ship utilizing a hull vane®: A case study of a hard-chine crew boat. *CFD Letters*, *12*(2), 95-105.

Saldana, M., Gallegos, S., Gálvez, E., Castillo, J., Salinas-Rodríguez, E., Cerecedo-Sáenz, E., ... & Toro, N. (2024). The Reynolds number: A journey from its origin to modern applications. *Fluids*, *9*(12), 299.

Sasvia, H. (2019). Penegakan Hukum Perikanan di Wilayah Laut Indonesia. *Lex Scientia Law Review*, *3*(2), 227-234.

Shi, G., Priftis, A., Xing-Kaeding, Y., Boulougouris, E., Papanikolaou, A. D., Wang, H., & Symonds, G. (2021). Numerical investigation of the resistance of a zero-emission full-scale fast catamaran in shallow water. *Journal of Marine Science and Engineering*, *9*(6), 563.

Siagian, J. M. G., Zakky, A. F., & Iqbal, M. (2020). Kajian Kekuatan Struktur dan Buckling pada Livestock Carrier Catamaran 1500 DWT dengan Metode Elemen Hingga. *Jurnal Teknik Perkapalan*, *8*(3), 360-367.

Siddiqui, S. A., Singh, S., Bahmid, N. A., & Sasidharan, A. (2024). Applying innovative technological interventions in the preservation and packaging of fresh seafood products to minimize spoilage-A systematic review and meta-analysis. *Heliyon*, *10*(8), e29066.

Tavares, J., Martins, A., Fidalgo, L. G., Lima, V., Amaral, R. A., Pinto, C. A., ... & Saraiva, J. A. (2021). Fresh fish degradation and advances in preservation using physical emerging technologies. *Foods*, *10*(4), 780.

Wheeler, M. P., Matveev, K. I., & Xing, T. (2021). Numerical study of hydrodynamics of heavily loaded hard-chine hulls in calm water. *Journal of Marine Science and Engineering*, *9*(2), 184.

Xing-Kaeding, Y., & Papanikolaou, A. (2021). Optimization of the propulsive efficiency of a fast catamaran. *Journal of Marine Science and Engineering*, *9*(5), 492.

Zeng, Q., Hekkenberg, R., & Thill, C. (2019). On the viscous resistance of ships sailing in shallow water. *Ocean Engineering*, *190*, 106434.

Zhu, C., Chi, Z., Bi, C., Zhao, Y., & Cai, H. (2019). Hydrodynamic performance of floating photobioreactors driven by wave energy. *Biotechnology for Biofuels*, *12*(1), 54.